One-step production of highly monodisperse size-controlled poly(lactic-co-glycolic acid) nanoparticles for the release of a hydrophobic model drug

Javid Abdurahim, Christophe Serra, Christian Blanck, Madeline Vauthier

Version of Record: https://www.sciencedirect.com/science/article/pii/S1773224722002684
Manuscript_d3dad0f9b8afeff9a856fed5dec0e60d

One-step Production of Highly Monodisperse Size-Controlled Poly(lactic-co-glycolic acid) Nanoparticles for the release of a hydrophobic model drug

Javid Abdurahim, Christophe A. Serra*, Christian Blanck, Madeline Vauthier*
Université de Strasbourg, CNRS, Institut Charles Sadron UPR 22, F-67000 Strasbourg, France

Abstract
Biodegradable polymeric nanoparticles are considered as promising drug delivery systems due to their high potential in tuning the release and alleviate side effects. However, particle greater than 200 nm can be detected by the immune system. Thus, this paper focuses on the elaboration of size-controlled nanoparticles of poly(lactic-co-glycolic acid) smaller than 200 nm encapsulating a model drug. For this purpose, the biodegradable polymer was first solubilized in ethyl acetate and then dispersed into water by different nanoemulsification devices: shear mixer, sonicator and elongational-flow reactor and micromixer. Last two devices showed the capacity to produce monomodal nanoparticles of targeted size range at different continuous to disperse phase volume ratios. On a second part, nanoparticles produced with the micromixer were employed as nanocarriers for rifampicin, a hydrophobic antibiotic. These drug-loaded nanoparticles were produced at different drug concentrations to study the effect of drug load on the particle properties. Different techniques such as dynamic light scattering, transition electron microscopy and ultraviolet spectroscopy were employed to thoroughly characterize the nanoparticle diameter, size dispersity and morphology, drug encapsulation efficiency and *in vitro* drug release profile. Nanoparticles produced with the micromixer, following a new phase pre-saturation approach, had a highly monomodal diameter as low as 63 nm and an encapsulation efficiency of 40% at 5% w/v drug load was measured. Drug release tests under sink conditions showed 44% ± 2% cumulative drug release within 8 days.

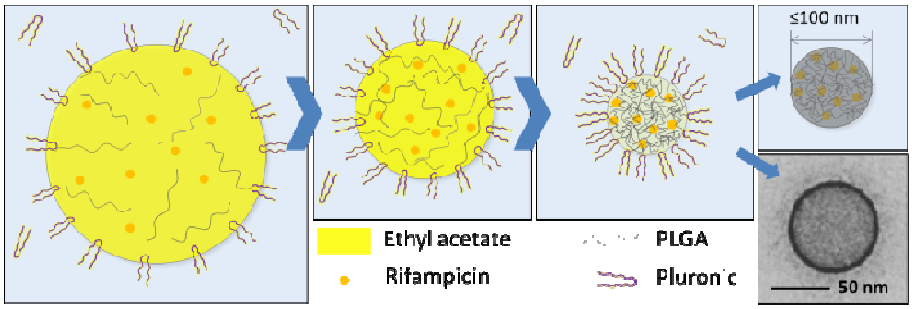

Keywords: poly(lactic-co-glycolic) acid, rifampicin, polymeric nanoparticles, encapsulation, *in vitro* drug release

1. Introduction

The need for a new drug delivery system is requested by the pharmaceutical industry (Barba *et al.*, 2020; Noël *et al.*, 2019). Indeed, the number new drugs of class IV from biopharmaceutical classification system and drugs having a continuous dose requirement for treatment, without harming organs, have triggered the need for alternative drug delivery strategies (Abdelaziz *et al.*, 2018; Boyd *et al.*, 2019). Some diseases request to maintain an effective therapeutic drug concentration over time and thus to develop formulations that allow the prolonged delivery of an active pharmaceutical ingredient (Liu *et al.*, 2019; Mei *et al.*, 2018). Previous studies suggest that drugs having delivery issues could be encapsulated in biodegradable polymeric nanoparticles (NPs) of diameters as low as 200 nm to improve stability of drugs and to tune their release profiles (Bulmer, 2012; Cheng *et al.*, 2016; Ding *et al.*, 2019a). Indeed, biodegradable polymers have the capacity of being cleaved into biocompatible byproducts through enzymatic degradation and enzyme-catalyzed hydrolysis process, thus delivering drugs in a controlled release manner (Liu *et al.*, 2019; Park *et al.*, 2005). Poly(lactic-co-glycolic acid) block copolymer (PLGA) is one of the carrier candidates for drug delivery systems since European Medicine Agency and Food and Drug Administration approved it for its bioavailability (Elmowafy *et al.*, 2019; Sun *et al.*, 2012; Allahyari *et al.*, 2020). This biocompatible polymer can protect drugs from degradation until its release starts (Mahboubian *et al.*, 2010; Mora-Huertas *et al.*, 2010). To study drug release kinetics from the system, it's also necessary to understand the

physicochemical properties of PLGA, such as the effect of molecular weight and the molar ratio of lactic and glycolic acid on its biodegradation rate. Indeed, the hydrolysis of PLGA, leading to lower molecular weight, is the key factor for the polymer's degradation process (Kamaly *et al*., 2016; Wang *et al*., 2000). Linear structure of PLGA makes polymer chains more mobile as the molecular weight decreases, resulting in faster diffusion of drug through the polymer matrix (Liggins and Burt, 2001). In this context, drug-loaded PLGA microspheres (57 µm of diameter) can easily be fabricated by the emulsification-evaporation method and encapsulation efficiency of 92% (1.5% w/w drug load) can be reached at optimum conditions (Mei *et al*., 2018; Mahboubian *et al*., 2010; Mei *et al*., 2018). However, disproportionately fast droplet surface hardening may occur during emulsification, limiting the polymer shrinkage. This hardening can be delayed by applying the pre-saturation method, *i.e.* by saturating the continuous phase with the disperse phase's solvent, in order to control the diffusion of organic solvent during its evaporation. Also, a presence of glycerides, such as Miglyol, can reduce diffusion of drug out of the polymer molecules (Wischke, 2008).

Moreover, based on the control over their morphology, size, bioavailability and high biostability, polymeric NPs are promising candidates as drug carriers (Mahboubian *et al*., 2010; Wallyn *et al*., 2018). While various methods such as emulsification-evaporation, salting-out or nanoprecipitation have been studied to produce NPs (Ding *et al.*, 2019a; Rafiei and Haddadi, 2019; Singh *et al.*, 2017), microfluidic-assisted processes appear to be an asset for the production of NPs with biological-related applications (Ding *et al.*, 2018; Vauthier and Serra, 2021). Indeed, size-controlled droplets can be generated even with highly viscous solutions (e.g. polymers) with viscosity ratios higher than 4, which is the limiting value according to Grace's theory for the shear devices (Anton *et al*., 2012; Taylor and Grace, 2009). Using these methods, the required drug carrier mass can be reduced in order to decrease production costs (Bulmer, 2012; Ding *et al*., 2019a). For instance, some of these systems have been developed by a two-step process to produce ketoprofen-loaded poly(methyl methacrylate) NPs (45% of encapsulation efficiency) with controlled size (100 to 200 nm). Selecting an appropriate encapsulation technique is an important stage while working with biodegradable polymers. However, the techniques presented in the literature for emulsification are still usually multistep multiplying risks of contaminations and drug alteration (Ding *et al*., 2019a, 2019b, 2018).

This work thus proposes to implement the emulsification-evaporation method for the one-step production of PLGA drug-loaded NPs. Influence of three different emulsification devices operating parameters (emulsification time, temperature and mixing parameters) as well as chemical parameters (drug concentration) on the nanoparticles' mean diameter and drug release profiles was thoroughly studied.

The main objectives of this work are to develop polymeric NPs having a specific size range (between 50 nm and 200 nm) and a low value of size dispersity through process optimization. These make NPs capable of encapsulating a drug (rifampicin) with a sufficient drug load in a one-step process for a later drug delivery at reduced side effects. Three different devices (sonicator, shear mixer and elongational-flow reactor and micromixer) are investigated to elaborate an efficient approach to develop highly stable oil-in-water nanoemulsions that upon evaporation-induced nanoprecipitation will be converted into proper drug delivery systems. Since an increase in drug load may lead to some alterations, such as a bulk erosion of PLGA in acidic medium, *in vitro* drug release studies by maintaining sink conditions at different drug loads are presented. It should also be considered that, the concentration of the drug in a medium can change the degradation kinetics (Friederike von Burkersrodaa, 2002; Sadouki, 2020). Moreover, compared to previous works done with polymeric NPs (Ding *et al*., 2018; Hernández-Giottonini *et al*., 2020; Singh *et al*., 2017), in this work the continuous phase pre-saturation is applied for the first time to the microfluidic-assisted emulsification and solvent-evaporation

method in order to i) increase the amount of encapsulated hydrophobic model drug (rifampicin) and ii) improve the control over NP diameter and size distribution.

2. Materials and methods

2.1. Materials

Poly(lactic-co-glycolic acid) 50:50 (PLGA) block copolymer Resomer® RG 504 H (Merck, Mw = 64 kg/mol, stored at 4°C), ethyl acetate (Merck), Pluronic® F-127 (Merck) as a non-ionic surfactant and Miglyol® 812, a medium-chain triglyceride (Caelo) were used as received to prepare the emulsions. Rifampicin (TCI Chemicals, stored at 4°C), citric acid monohydrate (Merck), anhydrous sodium carbonate (Merck) and Spectrum™ Spectra/Por™ 4 RC dialysis bag tubing (molecular weight cutoff between 12,000 and 14,000 g/mol) were purchased in order to proceed drug encapsulation/release.

2.2. Preparation of nanoemulsions

The disperse phase was composed of 1% w/v of PLGA (and if needed a given amount of rifampicin) solubilized in ethyl acetate. The continuous phase was composed of 1.5% w/v of surfactant solubilized in deionized water. 8.7% v/v of ethyl acetate were introduced in continuous phase to apply the pre-saturation method.

Samples at various continuous/disperse phases (C/D) volume ratios were emulsified by shear mixing, sonication and elongational-flow micromixing at room temperature. After emulsification operations, all samples were left overnight in a fume hood to let the polymers' solvent evaporated and the polymer to nanoprecipitate.

Shear mixing: a rotor–stator mixer (Ultra-Turrax® T 25 basic, 800 W, IKA®) having a 13 mm diameter arm was employed for high-energy homogenization at six different rotational speeds. The continuous and the disperse phases, for a total volume of 15 mL, were homogenized at different speeds for a given emulsification time at 20°C.

Sonication: an ultrasonic homogenizer (Bandelin Sonopuls HD2200) having a 3 mm diameter tip was used to emulsify two immiscible phases during a given time at different amplitudes (t_{on}/t_{total}) to produce stable emulsions. A cooling water bath was applied to maintain the temperature at 20^{o}C.

Elongational-flow micromixing: a reactor micromixer (µRMX) consisted in two mid pressure syringe pumps (neMESYS® Mid Pressure Module, Cetoni), two 25 mL stainless steel syringes (Cetoni) and one poly(etheretherketone) tee (Valco Vici) was employed for the production of nanoemulsions. The syringe pumps were connected and operated by the supplier's software in order to operate both pumps at the same reciprocating flow rate. By using this technique, liquid phases can be independently injected or withdrawn a given number of times. The micromixer was composed of a microchannel of 0.15 mm diameter linked to the stainless-steel syringes by two poly(tetrafluoroethylene) tubings (1.06 mm ID, 1.68 mm OD), acting as a restriction to the flow.

2.3. Production of PLGA drug-loaded nanoparticles

In order to start encapsulation, a given amount of drug (rifampicin) was first mixed to 10 µL of Miglyol® 812 (to improve the encapsulation efficiency and decrease the drug burst release) and then added to 1% w/v PLGA in

ethyl acetate, the resulting solution composing the oil disperse phase. The continuous phase was composed of water saturated with 8.7% v/v ethyl acetate so as to prevent the drug diffusion from oil to the aqueous phase (Wischke and Schwendeman, 2008). After the successful production of nanoemulsions, all samples were left overnight in a fume hood to let the solvent evaporate and a nanosuspension of drug-loaded PLGA NPs in water was recovered.

To separate the drug-loaded nanoparticles (DNPs) from water phase, in order to calculate the encapsulation efficiency and to study the cumulative drug release from the DNPs under sink condition, nanosuspensions were first centrifuged at 9500 rpm during 30 min at 20°C (Rotina 420R Hettich Zentrafugen) in order to eliminate surfactant and then lyophilized (Labconco Freezone freeze dryer) at 0.4 mbar during 24 h at -50°C.

2.4. Characterization methods

2.4.1. Determination of particle size and size distribution

The z-average diameter and size distribution of the NPs were assessed by dynamic light scattering (DLS) using a Nano ZetaSizer instrument (Malvern). The helium-neon laser (4 mW) was operated at 633 nm, the scatter angle was fixed at 173° and the sample temperature was maintained at 25°C.
The polydispersity index of the particle size (PDI) was a measure of the broadness of the size distribution and it was commonly admitted that PDI values below 0.2 corresponded to monomodal distributions (Anton *et al*., 2012; Ding *et al*., 2016, Vauthier *et al.*, 2021). Analyses of nanoparticles' diameter were performed by pouring dropwise 0.02 mL of the nanosuspensions into 1 mL of deionized water. Measurements were conducted in triplicates, each measurement being an average of 30 values calculated by the ZetaSizer.

2.4.2. Drug load and encapsulation efficiency

The drug load (DL) and the encapsulation efficiency (EE) were calculated according to Equation 1, 2 (Chourasiya *et al*., 2016; Khan *et al*., 2013). DL corresponds to the drug weight percentage in the final product, EE is the weight ratio of encapsulated drug to the total weight of drug introduced in the feed.

DL = weight of encapsulated drug / weight of the DNPs (1)

EE = weight of encapsulated drug / weight of drug introduced in the device (2)

2.4.3. Drug release from PLGA drug-loaded nanoparticles

DNPs were first loaded into a dialysis bag tubing, then the bag was immersed in a 60 mL of pH-controlled phosphate buffer solution (pH = 7.4). Following this, rifampicin release from polymeric DNPs was realized in an incubator (PolyMax 1040, 330 W, Heidolph) equipped with a temperature control system (37°C), a sample collection platform and a rotational speed controller (50 rpm).

The cumulative drug release in time was calculated with Equation 3, 4 by taking the drug loss into account.

$$T_n = (\lambda_n^{332} / \lambda^{332})\, C_0 + L \quad (3)$$

with T the total released drug (µg) at time n, λ_n^{332} the absorbance at time n, λ^{332} absorbance at certain drug quantity (µg/mL) C_0 obtained from the calibration curve, and L, total loss of drug at a phosphate buffer solution replacement (µg).

Drug release = T_n / Weight of drug loaded (4)

The standard deviation (SD) of the cumulative drug release in time was calculated with Equation 5.

$$SD = \sqrt{\frac{\sum_{i=1}^{j}(x_i - \bar{x})^2}{j-1}} \quad (5)$$

with j the number of experimental values, x_i the drug release value of experiment i (calculated with Equation 4) and $\bar{x}$ the average value of the j x_i values. For the current work, j = 5.

2.4.4. Transmission electron microscopy

To analyze the morphology and shape of the nanoparticles, transmission electron microscopy (TEM) experiments were performed. 5 µL of the nanosuspensions were deposited onto a freshly glow discharged carbon-covered grid (400 mesh). The suspension was left for 2 minutes and then the grid was negatively stained with 5 µL of uranyl acetate (2% v/v in water) for another minute before being dried using a filter paper. The grids were observed at 200 kV with a Tecnai G2 (FEI) microscope. Images were acquired with an Eagle 2k (FEI) ssCCD camera.

The images acquired from TEM were separately analyzed by ImageJ Java-based image processing program. Following this, 500 size measurements were realized and the statistical analysis was done generating Gaussian curves.

2.4.5. UV-visible spectroscopy

Ultraviolet-visible spectroscopy (Perkin Elmer – Lambda 25) with a wavelength ranging from 2500 nm to 190 nm was used to quantify the drug concentration that was encapsulated in the nanoparticles and released from the drug-loaded NPs. 3.5 mL standard quartz cuvette with 10 mm light path was used for all characterizations.

2.4.6. Interfacial tension measurements

The interfacial tensions between oil and water phases were measured by employing Teclis Scientific Tracker device according to the rising bubble method. First, water phase (deionized water and surfactant) in a 25 mL glass cuvette was placed inside the temperature-controlled chamber at 20°C. Oil phase was then continuously injected from a 500 µL glass syringe directly to the center of water solution to create and to maintain a 3 µL droplet.

3. Results and Discussions

3.1. Production of biodegradable PLGA nanoparticles

In a first part, the production of biodegradable nanoparticles (NPs) with poly(lactic-co-glycolic acid) (PLGA) was conducted with three different devices: rotor-stator mixer, sonicator and elongational-flow micromixer (µRMX). The goal here was to assess the effect of operating processing parameters (emulsification time and mixing parameter) and chemical parameters (continuous to disperse phase C/D volume ratio) on the NPs' size and size dispersity. Emulsification times and mixing parameters (MP) employed are given in Table 1. Results obtained by DLS are presented for the three devices in Figure 1.

Table 1. Parameters used to produce PLGA NPs with three different emulsification devices.

Device	Emulsification times (min)	Mixing parameter (MP)	C/D volume ratio

Rotor-stator mixer	5 to 25	6,500 to 24,000 rpm	60/40 and 85/15
Sonicator	1 to 12	10% to 90% of amplitude	60/40 and 85/15
µRMX	20 to 100[†]	10 to 40 mL/min	60/40 and 85/15

[†]60 min corresponds to 150 cycles

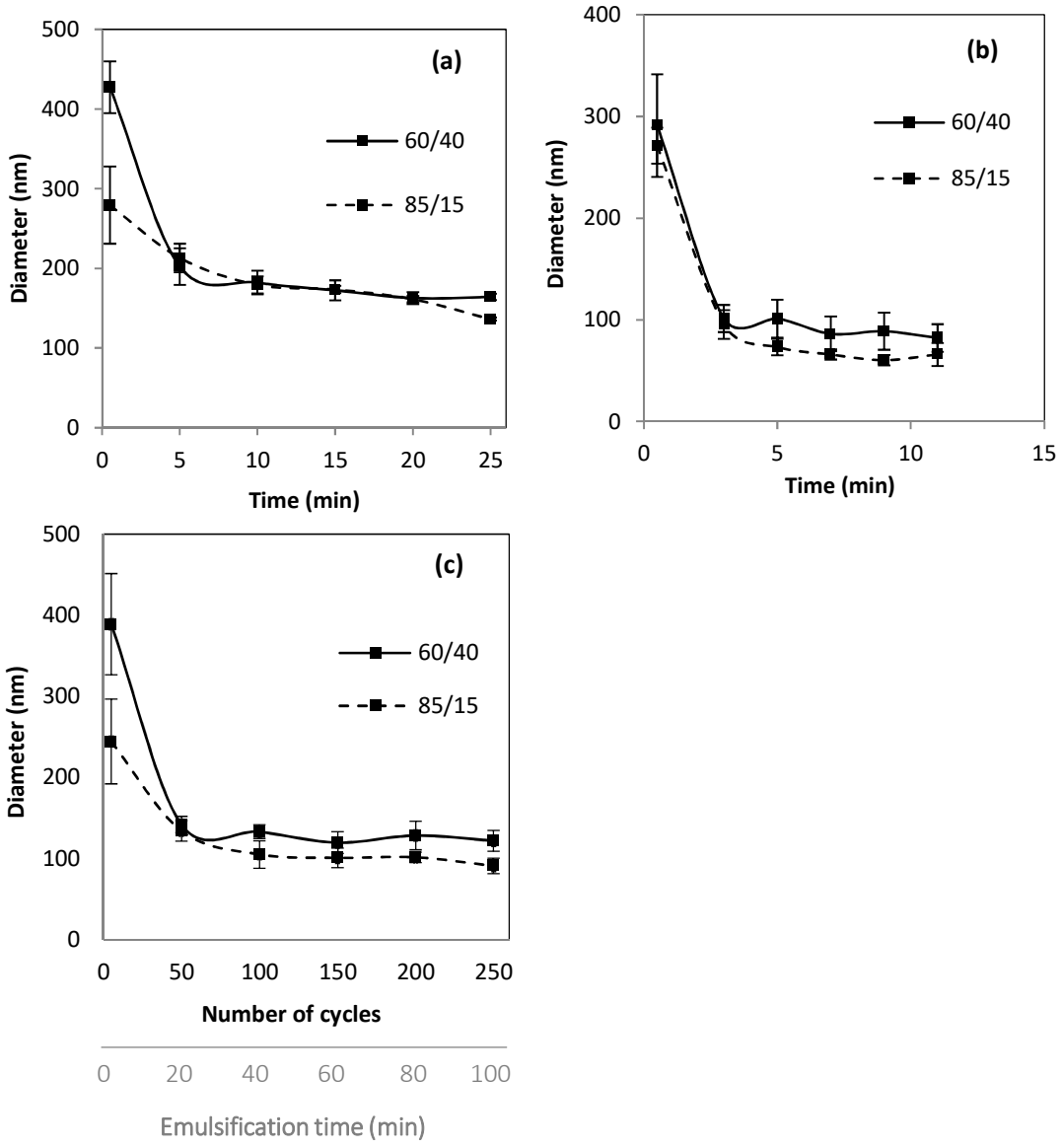

Figure 1. Evolution of PLGA nanoparticles' size at 85/15 and 60/40 volume ratios. The PLGA NPs were produced by a) rotor-stator mixing, b) sonication or c) elongational-flow micromixer.

After a short emulsification time (less than 5 min), there were huge size differences between the three devices. With C/D = 60/40 for example, highly polydisperse particles of 430 nm, 300 nm and 400 nm were produced by the rotor-stator mixer, the sonicator and the elongational-flow reactor and micromixer (µRMX) respectively (Figure 1, Figure S1). These results, due to the different mechanisms of particle formation, were coherent with previous

study carried out by our team (Anton *et al*., 2012; Vauthier *et al*. 2021). Indeed, rotor-stator produced particles by shear effect applied by external rotational force, sonication process produced particles by water gas bubble implosion (known to lead to smaller particles) and µRMX mainly used a flow focusing mechanism in order to produce nanodroplets. After a longer emulsification time, a plateau value was obtained at lower sizes: 150 nm (shear mixer) and 100 nm (sonicator and elongational-flow reactor and micromixer). The operating parameters of shear mixer, sonicator and elongational-flow reactor and micromixer also allowed optimizing NPs' size and PDI value. These parameters are rotation speed, amplitude and flow rate respectively (Figure S2). The minimum size was 136 nm with the rotor-stator mixer (25 min, 17500 rpm), 57 nm with sonicator (5 min, 70% amplitude) and 80 nm with the elongational-flow reactor and micromixer (60 min, 40 mL/min). The emulsification with sonicator at 5 minutes, 70% amplitude conditions reached 70°C temperature within first 3 minutes without an external cooling condition.
Moreover, with a higher C/D volume ratio (85/15), the average particle size decreased more than 20% in size, as reported in Figure 1.b.c and in Figure S2.b.c. This was coherent with previous studies demonstrating that decreasing the polymer concentration, *i.e.* increasing the C/D volume ratio, decreased the system's viscosity which lead to the production of smaller particles (Anton *et al*., 2012; Bally *et al*., 2012).
All devices allowed thus the production of monomodal nanoemulsions (PDI below 0.2) of PLGA with a size below 150 nm that can mainly be controlled by operating parameters.

Finally, it should be mentioned that ultrasound effects like cavitation raised during ultrasonication process. Cavitation leads to high temperatures (t≥60°C, Figure S3) that can later affect the drug stability and accelerate the polymer degradation. However, shear mixing showed that NPs could be produced at controlled temperatures, but the size of produced NPs was bigger, which was not suitable for the drug encapsulated systems. On the opposite, the µRMX did not induce any temperature increase and thus was the only device chosen to further study the one-step encapsulation of rifampicin.

3.2. Drug encapsulation inside biodegradable nanoparticles

In the previous part, three different devices have been studied to produce biodegradable NPs, showing suitable size and dispersity features for drug delivery systems. However, by shear mixing and by sonication unnecessarily high heat effects occurred. Since µRMX performed no excess heat release and produced monomodal polymeric NPs, this device has been chosen (150 cycles, 30 mL/min) for the following investigation concerning drug encapsulation by PLGA NPs.

In this part, the influence of drug (rifampicin) concentration on its encapsulation efficiency was investigated. For this purpose, the drug was introduced into the disperse phase at different weight contents with respect to PLGA, ranging from 1%/PLGA w/w to 10%/PLGA w/w (the samples were called R1 to R10 respectively) and the resulting drug-loaded nanoparticles (DNPs) were analyzed by UV-visible spectroscopy at 332 nm after establishing a calibration curve (Figure S4).

DNPs size and PDI variations with respect to the initial drug weight content are presented in Figure 2 while DL, EE, amount of encapsulated drug (µg) and the average size of a drug carrier are reported in Table 2.

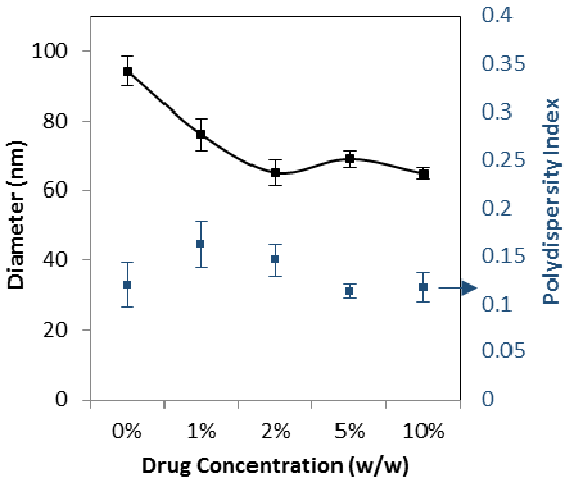

Figure 2. Evolution of the PLGA drug-loaded nanoparticles' diameter size and polydispersity index for different drug weight contents with respect to PLGA.

Table 2. Drug loading (DL) and encapsulation efficiency (EE) for different initial drug weight contents.

Sample name	Initial drug weight content with respect to PLGA (w/w)	DL (%)	EE (%)	Encapsulated Drug (µg)	Average Size of DNP
R1	1%	2.2 ± 0.1	95 ± 3	191 ± 5	76 ± 5
R2	2%	3.6 ± 0.2	80 ± 5	319 ± 19	66 ± 4
R5	5%	4.5 ± 0.5	40 ± 3	395 ± 27	69 ± 2
R10	10%	7.2 ± 0.4	32 ± 2	634 ±33	65 ± 2

Increasing rifampicin initial weight content unexpectedly decreased the NPs' size from 94 ± 4 nm down to 69 nm ± 2 nm (Figure 2). This result was explained by a decrease in the interfacial tension between the continuous and disperse phases without ($\sigma_{0\%}$= 3.2 mN/m) and with drug at 5% w/w weight content with respect to PLGA ($\sigma_{10\%}$= 2.8 mN/m), due to the intermolecular interactions that occur between PLGA and rifampicin and due to the presence of rifampicin at the surface of the droplets (Figure S5). Moreover, the DL increased from 2.2% to 7.2% while increasing the initial drug concentration from 1% w/w to 10% w/w. EE reached its highest value at the lowest drug load, however the mass quantity of encapsulated drug (191 µg at 1%/PLGA w/w) was the lowest value (319 µg at 2%/PLGA w/w, 395 µg at 5%/PLGA w/w and 634 µg at 10%/PLGA w/w) among all experiments. The minimum load could be applied to minimize the loss of (non-encapsulated) drug, however the highest quantity of encapsulated drug, considering the drug/polymer ratio, can be reached only at higher initial drug loads (Table 2). So, it appeared that, considering the size and PDI values, 5% w/w initial drug concentration regarding to polymer weight content, led to the production of the most monomodal DNPs having a diameter below 70 nm.

3.3. Influence of the initial drug weight content on the drug release

In order to study the drug release at 37°C from previously produced DNPs, they were isolated from the solution by centrifugation (9500 rpm, 30 min) and filtration (filter diameter = 0.2 µm) before being introduced into a

dialysis tube in a 7.4 pH-controlled buffer solution. The amount of drug (µg) released from DNPs was determined by UV-visible spectroscopy at 332 nm by taking into account the rifampicin possible degradation (Equation 3) (Sadouki, 2020) and the cumulative drug release was calculated by the mass ratio of the released drug to the initially loaded drug (Equation 4).

Drug release kinetics for different initial drug weight contents with respect to PLGA are given in Figure 3. R1, R2, R5 and R10 represent the samples studied at 1% w/w, 2% w/w, 5% w/w and 10% w/w of initial drug introduced in the disperse phase respectively. It is worthy to note that the given Rifampicin released percentage values were calculated considering the encapsulated drug quantity. For example, a quantity of encapsulated drug for R5 was 395 ± 15 µg, and 175 ± 9 µg was released after 8 days, which makes 45% of drug released.

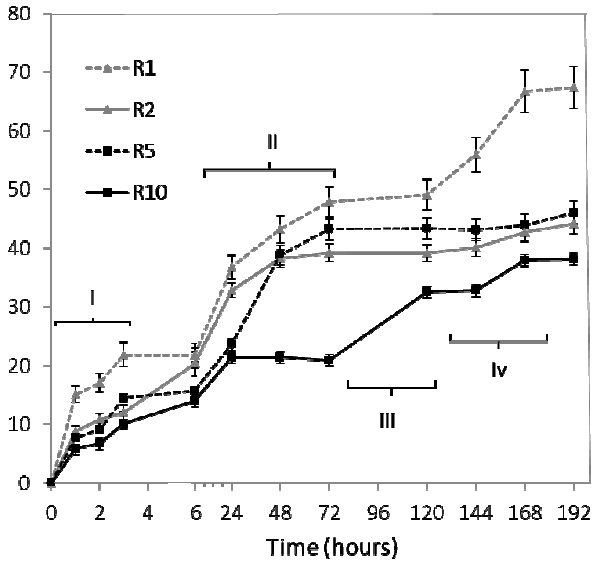

Figure 3. *In-vitro* drug release profiles and their four substages (i, ii, iii and iv) at 1% w/w (R1), 2% w/w (R2), 5% w/w (R5), and 10% w/w (R10) rifampicin/polymer weight content.

First of all, the amount of released drug increased with time, proving that the developed system achieved a sustain drug release over time. Moreover, the drug quantity released in 8 days was 129 ± 12 µg (67%), 147 ± 10 µg (46%), 175 µg ± 9 µg (45%) and 242 µg ± 9 µg (38%) for R1, R2, R5 and R10 respectively. So, different drug release kinetics occurred for a maximum amount of Rifampicin released in 8 days equal to 242 µg. This drug delivery system can thus be adapted to various released doses. Observing the error bars, DNPs formed with the lowest initial drug concentration (R1) may be considered as a non-stable system, contrary to DNPs produced with higher drug concentrations. More interestingly, in Figure 3, four substages were identified for drug release process: (i) burst release effect was noticed within first 3 hrs; (ii) from 6 to 72 hrs, a cumulative drug release due to constant diffusion from DNPs to water was observed ; (iii) a partial resilience occurred between 3 and 5 days, which can be explained by the drug entrapment near inner surface of DNPs; (iv) on last stage, the drug encapsulated in center of DNPs started to diffuse into water after reaching DNPs' surface.

These four substages are likely correlated either to the polymer degradation or to diffusion of drug across PLGA chains. In order to investigate this point, transmission electron microscopy images were carried out the first, third and eighth days of release study (Figure 4). DNPs investigated by TEM were at 5% w/w initial drug weight content due to high accuracy in diameter and size distribution, as demonstrated in Figure 2.

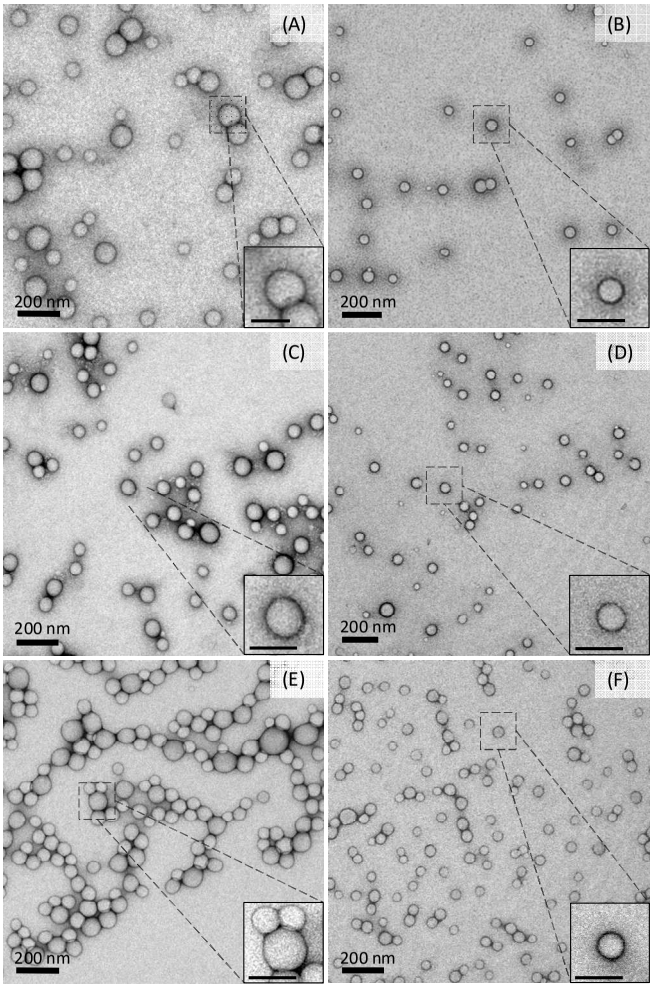
(A)
(B)
(C)
(D)
(E)
(F)
200 nm

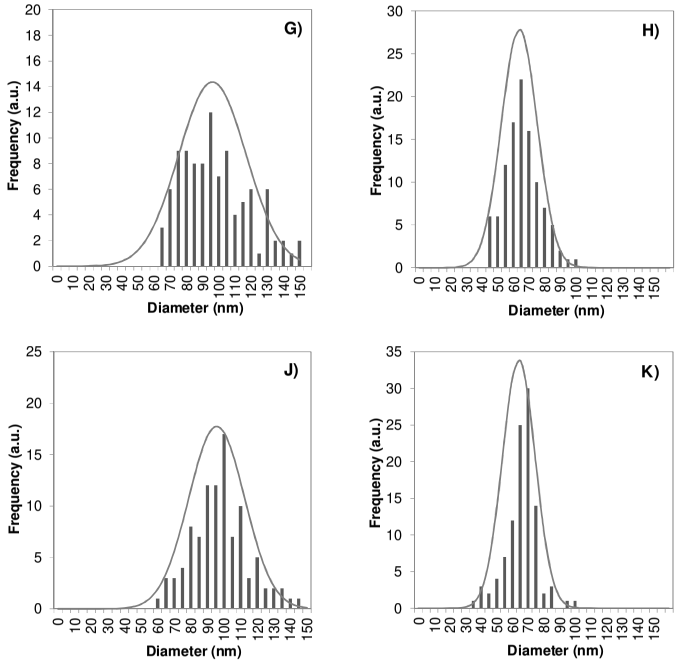
G)
H)
J)
K)
Frequency (a.u.)
Diameter (nm)

Figure 4. TEM images (A-F) and statistical analysis (G-K) of unloaded PLGA NPs (A, C, E, G, J) and 5% w/w drug-loaded DNPs (B, D, F, H, K) after 1st (A, B), 3rd (C, D) and 8th day (E, F). The statistical analysis of PLGA NPs (G, J) and DNPs (H, K) diameters is presented for the 1st day (G, H) and after 8 days of incubation (J, K) at 37^{0}C and pH = 7.4).

In Figure 4, TEM images showed spherical NPs for unloaded PLGA NPs and through all *in vitro* release period. From the initial stage, NPs (A) and DNPs (B) produced with the same operating parameters had a size difference of more than 30 nm. Thus, diameter size difference between unloaded NPs (G, 98 nm) and DNPs (H, 64 nm) at the first day confirmed the previously discussed DLS size results (Figure 2). The broader Gaussian curve obtained for the PLGA NPs also proved the higher PDI compared to DNPs. The blank NPs at 3rd day (C), and at 8th days (E) showed, by TEM, a high morphological stability property similar to DNPs at 3rd day (D), and at 8th day (F), and the statistical analysis (G-K) confirmed these results.

As previously discussed in the literature, PLGA 50:50 degradation can start after more than 2 weeks (Allahyari *et al.*, 2020) and here, PLGA-based NPs were still spherical and without physical damages after 8 days. This phenomenon made a clear understanding of the mechanism of drug release that occurred: rifampicin was released from the DNPs by diffusion between PLGA chains.

Overall, no PLGA degradation was observed within 8 days, which makes a diffusive drug release understandable. For further studies the drug release can be improved through polymer degradation.

4. Conclusion

Emulsification-evaporation method was a reliable way to produce biodegradable, biocompatible poly(lactic-co-glycolic acid) nanoparticles (PLGA NPs). First, processes as sonication, shear-mixing and elongational flow micromixing were operated and allowed the production of smaller NPs (diameter below 150 nm). Indeed, by changing emulsification time and mixing parameters, minimum values of diameter size and size distribution (PDI below 0.2) have been obtained. The minimum size was 136 nm with the rotor-stator mixer (25 min, 17500 rpm), 57 nm with sonicator (5 min, 70% amplitude) and 80 nm with the elongational-flow reactor and micromixer (60 min, 40 mL/min). It was thus stated that elongational-flow micromixing was the most reliable way to produce biocompatible, monomodal NPs adapted for drug encapsulation with fine size control.
Rifampicin was then encapsulated into PLGA NPs at different drug loads ranging from 1% w/w to 10% w/w regarding of polymer weight content. Interestingly, the unloaded PLGA NPs and drug-loaded NPs had different diameter size values, respectively 94 nm and 63 nm. Considering DNPs diameter and size dispersity, the optimum EE of 40% at 5% w/w initial drug concentration was achieved. Additionally, the continuous phase pre-saturation method was applied to 60/40 continuous/disperse phases before elongational-flow emulsification which decreased the size of NPs from 126 nm to 94 nm without drug encapsulation. TEM images showed the difference between size, monomodality of unloaded and drug loaded NPs and a non-degradable characteristic of the PLGA matrix within 8 days.
In vitro drug release study from spherical polymeric DNPs under sink conditions showed that the drug quantity can be controlled by varying the initial drug weight content but simultaneously affects DNPs' average size. Moreover, the cumulative release reached higher values with an increasing amount of initial drug weight content. Encapsulated Rifampicin quantities inside PLGA DNPs were between 191 µg to 634 µg and the released drug quantities were equal to 129 µg (67%) and to 242 µg (38%) respectively.

This work thus opens innovative perspectives for the design of controlled drug release systems. Indeed, the influence of the polymer structure and molecular weight and the interrelation between the surface morphology

and the diffusion rate of a produced nanomaterial can be investigated in order to obtain an improved drug delivery.

Acknowledgements

The authors would like to thank Mélanie Legros and Marc Schmutz for the access to ICS characterization and electron microscopy platforms respectively. Drenckhan Wiebke and Jacomine Leandro are acknowledged for their support during the surface tension measurements while Jean Muller is thanked for his help in processing the NPs' size data. Special thanks are addressed to Campus France and French Embassy in Azerbaijan for research funding.

References

Abdelaziz, H.M., *et al*., 2018. Inhalable particulate drug delivery systems for lung cancer therapy: Nanoparticles, microparticles, nanocomposites and nanoaggregates. J. Control. Release 269, 374–392. https://doi.org/10.1016/j.jconrel.2017.11.036

Allahyari, M., *et al*., 2020. In-vitro and in-vivo comparison of rSAG1-loaded PLGA prepared by encapsulation and adsorption methods as an efficient vaccine against Toxoplasma gondii". J. Drug Deliv. Sci. Technol. 55, 101327. https://doi.org/10.1016/j.jddst.2019.101327

Anton, N., *et al*., 2012. A new microfluidic setup for precise control of the polymer nanoprecipitation process and lipophilic drug encapsulation. Soft Matter 8, 10628–10635. https://doi.org/10.1039/c2sm25357g

Bally, F., *et al*., 2012. Improved size-tunable preparation of polymeric nanoparticles by microfluidic nanoprecipitation. Polymer (Guildf). 53, 5045–5051. https://doi.org/10.1016/j.polymer.2012.08.039

Barba, A.A., *et al*., 2020. Engineering approaches for drug delivery systems production and characterization. Int. J. Pharm. 581, 119267. https://doi.org/10.1016/j.ijpharm.2020.119267

Boyd, B.J., *et al*., 2019. Successful oral delivery of poorly water-soluble drugs both depends on the intraluminal behavior of drugs and of appropriate advanced drug delivery systems. Eur. J. Pharm. Sci. 137, 104967. https://doi.org/10.1016/j.ejps.2019.104967

Bulmer, C., 2012. Encapsulation and Controlled Release of rHu-Erythropoietin from Chitosan Biopolymer Nanoparticles. Electronic Thesis and Dissertation Repository. 553. https://ir.lib.uwo.ca/etd/553

Cheng, Q., *et al*., 2016. The Promising Nanocarrier for Doxorubicin and siRNA Co-delivery by PDMAEMA-based Amphiphilic Nanomicelles. ACS Appl. Mater. Interfaces 8, 4347–4356. https://doi.org/10.1021/acsami.5b11789

Chourasiya, V., *et al*., 2016. Formulation, optimization, characterization and in-vitro drug release kinetics of atenolol loaded PLGA nanoparticles using 33 factorial design for oral delivery. Mater. Discov. 5, 1–13. https://doi.org/10.1016/j.md.2016.12.002

Ding, S., *et al*., 2016. Microfluidic nanoprecipitation systems for preparing pure drug or polymeric drug loaded nanoparticles: an overview. Expert Opin. Drug Deliv. 13, 1447–1460. https://doi.org/10.1080/17425247.2016.1193151

Ding, S., *et al*., 2018. Microfluidic-Assisted Production of Size-Controlled Superparamagnetic Iron Oxide Nanoparticles-Loaded Poly(methyl methacrylate) Nanohybrids. Langmuir 34, 1981–1991. https://doi.org/10.1021/acs.langmuir.7b01928

Ding, S., Serra, *et al*., 2019a. Production of dry-state ketoprofen-encapsulated PMMA NPs by coupling micromixer-assisted nanoprecipitation and spray drying. Int. J. Pharm. 558, 1–8. https://doi.org/10.1016/j.ijpharm.2018.12.031

Ding, S., *et al*., 2019b. Double emulsions prepared by two–step emulsification: History, state-of-the-art and perspective. J. Control. Release 295, 31–49. https://doi.org/10.1016/j.jconrel.2018.12.037

Elmowafy, E.M., *et al*., 2019. Biocompatibility, biodegradation and biomedical applications of poly(lactic

acid)/poly(lactic-co-glycolic acid) micro and nanoparticles, Journal of Pharmaceutical Investigation. Springer Singapore. https://doi.org/10.1007/s40005-019-00439-x

Friederike von Burkersrodaa, *et al*., 2002. Why degradable polymers undergo surface erosion or bulk erosion. Biomaterials 23, 4221–4231. https://doi.org/https://doi.org/10.1016/S0142-9612(02)00170-9

Hernández-Giottonini, K.Y., *et al*., 2020. PLGA nanoparticle preparations by emulsification and nanoprecipitation techniques: Effects of formulation parameters. RSC Adv. 10, 4218–4231. https://doi.org/10.1039/c9ra10857b

Kamaly, N., *et al*., 2016. Degradable controlled-release polymers and polymeric nanoparticles: Mechanisms of controlling drug release. Chem. Rev. 116, 2602–2663. https://doi.org/10.1021/acs.chemrev.5b00346

Khan, I.U., *et al*., 2013. Continuous-flow encapsulation of ketoprofen in copolymer microbeads via co-axial microfluidic device: Influence of operating and material parameters on drug carrier properties. Int. J. Pharm. 441, 809–817. https://doi.org/10.1016/j.ijpharm.2012.12.024

Liggins, R.T., Burt, H.M., 2001. Paclitaxel loaded poly(L-lactic acid) microspheres: Properties of microspheres made with low molecular weight polymers. Int. J. Pharm. 222, 19–33. https://doi.org/10.1016/S0378-5173(01)00690-1

Liu, J., *et al*., 2019. A modified hydrophobic ion-pairing complex strategy for long-term peptide delivery with high drug encapsulation and reduced burst release from PLGA microspheres. Eur. J. Pharm. Biopharm. 144, 217–229. https://doi.org/10.1016/j.ejpb.2019.09.022

Mahboubian, A., *et al*., 2010. Preparation and in-vitro evaluation of controlled release PLGA microparticles containing triptoreline. Iran. J. Pharm. Res. 9, 369–378. https://doi.org/10.22037/ijpr.2010.902

Mei, Q., *et al*., 2018. Formulation and *in vitro* characterization of rifampicin-loaded porous poly (ε-caprolactone) microspheres for sustained skeletal delivery. Drug Des. Devel. Ther. 12, 1533–1544. https://doi.org/10.2147/DDDT.S163005

Mora-Huertas, C.E., *et al*., 2010. Polymer-based nanocapsules for drug delivery. Int. J. Pharm. 385, 113–142. https://doi.org/10.1016/j.ijpharm.2009.10.018

Noël, F., *et al*., 2019. Design of a novel axial gas pulses micromixer and simulations of its mixing abilities via computational fluid dynamics. Micromachines 10, 1–16. https://doi.org/10.3390/mi10030205

Park, J.H., *et al*., 2005. Biodegradable polymers for microencapsulation of drugs. Molecules 10, 146–161. https://doi.org/10.3390/10010146

Rafiei, P., Haddadi, A., 2019. A robust systematic design: Optimization and preparation of polymeric nanoparticles of PLGA for docetaxel intravenous delivery. Mater. Sci. Eng. C 104, 1–11. https://doi.org/10.1016/j.msec.2019.109950

Sadouki, F., 2020. Micro-encapsulated poly (vinyl alcohol) nanoparticles for rifampicin delivery to the lungs. King's Coll. London.

Singh, Y., *et al*., 2017. Nanoemulsion: Concepts, development and applications in drug delivery. J. Control. Release 252, 28–49. https://doi.org/10.1016/j.jconrel.2017.03.008

Sun, Y., *et al*., 2012. Superparamagnetic PLGA-iron oxide microcapsules for dual-modality US/MR imaging and high intensity focused US breast cancer ablation. Biomaterials 33, 5854–5864. https://doi.org/10.1016/j.biomaterials.2012.04.062

Taylor, P., Grace, H.P., 2009. Dispersion Phenomena in High Viscosity Immiscible Fluid Systems and Application of Static Mixers As Dispersion Dispersion Phenomena in High Viscosity Immiscible Fluid Systems and Application O F Static Mixers As Dispersion Devices in Such Systems. Science (80). 6445, 37–41. https://doi.org/10.1080/00986448208911047

Vauthier, M., Serra, C.A., 2021. One-step production of polyelectrolyte nanoparticles. Polym. Int. 70, 860–865. https://doi.org/10.1002/pi.6178

Vauthier, M., Schmutz, M., Serra, C.A., 2021. One-step elaboration of Janus polymeric nanoparticles: A comparative study of different emulsification processes. Coll. Surf. A. 626, 127059. https://doi.org/10.1016/j.colsurfa.2021.127059

Wallyn, J., *et al.*, 2018. A new formulation of poly(MAOTIB) nanoparticles as an efficient contrast agent for in vivo X-ray imaging. Acta Biomater. 66, 200–212. https://doi.org/10.1016/j.actbio.2017.11.011

Wang, N., *et al.*, 2000. Synthesis,characterization,biodegradation,and drug delivery application of biodegradable lactic/glycolic acid polymers: I. synthesis and characterization. J. Biomater. Sci. Polym. Ed. 11, 301–318. https://doi.org/10.1163/156856200743715

Wischke, C., Schwendeman, S.P., 2008. Principles of encapsulating hydrophobic drugs in PLA/PLGA microparticles. Int. J. Pharm. 364, 298–327. https://doi.org/10.1016/j.ijpharm.2008.04.042